Scilight

Journal of Mechanical Engineering and Manufacturing
https://www.sciltp.com/journals/jmem

Article

A Review of Wear Mechanisms and Solutions Regarding Inserts for Grinding Applications

Naiara Poli Veneziani Sebbe [1,2,*], Andresa Baptista [1,3], Gustavo Pinto [1,3], Iván Iglesias [4] and Emanuel Thiago Oliveira [1]

[1] CIDEM, ISEP, Polytechnic of Porto, 4249-015 Porto, Portugal
[2] FEUP—Faculty of Engineering, University of Porto, 4200-465 Porto, Portugal
[3] LAETA-INEGI, Associate Laboratory for Energy, Transports and Aerospace, 4200-465 Porto, Portugal
[4] Defense University Center in the Spanish Naval Academy (CUD-ENM), Universidade de Vigo, Plaza de España, 36920 Marín, Spain
* Correspondence: napvs@isep.ipp.pt; Tel.: +351-22-83-40-500

How To Cite: Sebbe, N.P.V.; Baptista, A.; Pinto, G.; et al. A Review of Wear Mechanisms and Solutions Regarding Inserts for Grinding Applications. *Journal of Mechanical Engineering and Manufacturing* **2026**, *2*(1), 4. https://doi.org/10.53941/jmem.2026.100004

Received: 15 July 2025
Revised: 30 September 2025
Accepted: 9 October 2025
Published: 5 January 2026

Abstract: Cork has been one of the main pillars of the Portuguese economy for some decades and is today one of the most important natural materials exported from Portugal to the world. Nowadays, cork composites are used in products as diverse as sports flooring, wall memos, ladies' bags and shoes. However, these composites need to be processed and one of the first steps to produce cork granules is their grinding process. Although cork has a relatively low mechanical resistance and hardness, the degree of abrasion generated by cork on grinding pads during the grinding process is considerable. This study aims to determine which type of wear mechanisms are strongly associated with the premature end of life of grinding pads, which occurs due to reduced cutting efficiency and the generation of cork granules outside the specifications. This study will allow to understand the best ways to extend the useful life of tools and improving the cost/benefit ratio. The results obtained led to an understanding of the phenomena induced in the inserts and generated promising alternative solutions using special materials and coatings, allowing to improve the behaviour of the inserts against wear, making this operation more efficient and profitable.

Keywords: cork; cork grinders; grinders inserts; inserts wear; wear mechanisms; abrasion

1. Introduction

Cork is a natural material widely used since antiquity, namely in floating devices, however, recently has rapidly been gaining other important applications such as bottle stoppers for alcoholic beverages, in particular high-quality wines such as champagne and Port wine [1–4]. In the last century, the use of cork saw an important increase due to a new manufacturing approach: fabrication of cork agglomerates [5]. Furthermore, cork is narrowly related to the biodiversity maintenance as well as the sequestration of CO_2, being obtained from the outer bark of the oak tree [6,7]. Indeed, 2.3 million ha of cork oak forest distributed throughout the world is able to promote the retention of 14.4 million tons of CO_2 per year. Density of the cork can vary between 120 and 240 kg/m^3 depending on its porosity grade [8]. It is well known that one of the main quality indicators is the macroscopic porosity which depends on the prevalence of lenticular channels that cross cork planks radially [9].

Initially, cork was viewed only as the natural material that it is, allowing only to obtain products with relatively simple shape from the original cork oak skin, being bottle stoppers one of the most common applications [10,11]. However, this product requires a high level of quality and generates an appreciable amount of cork waste [12]. Furthermore, cork extracted from the cork oak with inferior quality should be driven to other application, making

the business more profitable. Thus, rapidly, the research linked to this kind of activity found new techniques in order to produce cork agglomerates [13] (cork composites), allowing the creation of a much wider range of products based on this material. Manufacturing processes associated to this new technique were also rapidly developed leading to make possible innovative design ideas. Nowadays, it is almost impossible to enumerate all the families of manufactured products based on cork material but, some of the most commons are sports floors, heat insulation for houses, sound insulation panels, cork boards and a huge number of articles related to household items or woman's fashion [14]. Furthermore, there are other relevant and potential applications with different objectives in areas such as healthcare and cosmetics [15], energy, automotive, aeronautical and aerospace applications [16], and it can also be used as a toxic biosorbent material [17].

However, production of cork agglomerates needs an initial basic, but very important operation: grinding process [18]. Knowing that cork extracted directly from the cork oak can bring several unexpected products, such as metallic parts that remain from cutting process, stones and other things, there is a need for the raw material to be filtered. This step enables the elimination of all foreign bodies with specific densities over the expected limit value as well as metal objects (with the use of metal detectors) in order to avoid their access to the grinding process thus, avoiding potential disastrous consequences to the equipment.

Cork grinders are huge machines provided with a special tool containing many inserts (usually about 144) assembled on a cylinder. The raw material is pulled and simultaneously grinded, transforming the initial material plates into granules. Although the cork is known as a soft material, the tool inserts are subjected to wear due to the friction between the inserts rotating at high speed and the raw material that is being pulled by the tool. The coefficient of friction between cork and steel can vary in the range of 0.2 to 1.2 [19], thus, wear is perfectly expected, and the inserts are naturally perceived as a consumable product. However, because this problem is perfectly restricted to cork composites producers and as this market is not as big as for instance the metal machining industry, research on the subject is not intense and tool wear is faced as a natural consequence of the grinding operation. Nevertheless, to make the process more effective and decrease the number of breakdowns caused by insert wear and loss of cutting efficiency (translated by the formation of coarser grain as final product), it is necessary to improve the wear behaviour of these inserts, studying the wear mechanisms and available ways to enhance the process effectiveness.

Knowing that the loss of mass by each insert is remarkable, it is important to analyse the types of wear that are affecting the insert surface, leading to define the best approach to try to solve the problem. Indeed, these kinds of inserts can follow two separate approaches: the use of a heat hardenable uncoated material or the use of a hard material as substrate, provided with a harder thin coating obtained usually by PVD (Physical Vapor Deposition) or CVD (Chemical Vapor Deposition) techniques [20]. However, the selection should be made as a function of the encountered wear mechanisms.

Due to the absence of previous work related to tool wear in cork grinding process, some similar situations were analysed, having help to discover how wear acts on the inserts surface. The desire of the scientific community to monitor the wear behaviour is relatively old. Effectively, and with focus mainly in quality issues, Fang et al. established a stochastic model based on 3D vibrations felt by tools to quantify wear groove formation on the tool surface [21]. As is cork grinding, the tool wear always affects the quality of the final product or process efficiency. In that study, the evolution of groove patterns is discussed, allowing observe that there are different mechanisms of formation and showing tool deterioration as a function of the parameters used in the process due to the concurrence of formation of new grooves or wipe-out of the initial grooves. Liu et al., studying the wear behaviour of different tools under HSM (High Speed Machining) conditions, identified as main patterns rake face wear, chipping, fracture and breakage as consequence of different phenomena such as mechanical friction, adhesion, diffusion and chemical wear, mainly promoted by cutting forces and high temperatures developed in the cutting area [22]. However, no conclusions were drawn about the preferred wear mechanisms observed in each kind of tool: CBN (Cubic Boron Nitride) tool, ceramic tool, coated carbide tool or fine-grained carbide tool, when machining cast iron and steel. Similar research was also developed by [23] regarding the machining of short carbon fibre reinforced plastic (SCFRP). In that study, authors observed two different wear stages during the cutting process: in the first stage rounding of cutting edges was observed and, after that, rake face wear. In this second stage, the wear rate begins to increase, and the wear pattern shifts from a rounding cutting edge to a massive rake face wear proceeding towards to the flank face, being possible to observe a rapid decrease in the rake angle. Abrasive wear was also observed on the tool surface translated by a groove in the middle of the tool, which can be explained by 3-body abrasive wear theory. Ultra-hard Polycrystalline Diamond (UHPCD) was also investigated by [24] in terms of wear ratio and corresponding wear mechanisms when employed in drilling tools used to grind granite. These authors found that the greater the hardness of the tool, the lower the rate of wear associated with, even in ultra-hard materials like PCD and UHPCD. Relatively to the wear pattern, PCD gradually fitted to the

ground material due to the grain loss of PCD. Composite materials dedicated to abrasion systems were also investigated by [25] but, in this case, due to a heterogeneous structure, the wear mechanisms are not exactly the same reported by the previously cited authors, having occurred grain abrasion, oxidation-abrasion, fatigue wear and adhesive wear.

Coated tools were also deeply investigated by different groups of authors in terms of wear mechanisms resulting from the contact during machining or other similar industrial processes, since coatings produced by HVOF-sprayed white cast iron [26] until others that, being already widely applied (TiN), remains as interesting issues due to new applications where they can be very useful [27].

In this work, due to the high hardness of the tools initial used and bearing in mind the large amount of mass loss by the same, coatings have not been considered due to the discontinuity of contact caused by the cork size heterogeneity. Thus, techniques as improving insert raw material and application of a heat treatment leading to improve hardness or the use of Metal Laser Sintering process to obtain more efficient inserts seems the best way to improve the inserts behaviour. Though, a deep investigation on the wear mechanisms shown on the insert surface was carried out, performing a comparative study between the conventional inserts used so far and the new ones obtained by different processes or using different alloys. Industrial grinding tests were carried out under a certain previously established period, containing in the same tool two distinct types of inserts, being then subjected to the same loads and remaining working conditions. Wear behaviour for both types of inserts where analysed, allowing taking conclusions relatively to their wear resistance under these conditions.

2. Materials and Methods

2.1. Materials

2.1.1. Substrate Characterization

The inserts used in the experimental work had an initial square shape of 40 × 40 mm^2. Conventional inserts were pre-machined to remove the cast skin. Three different types of inserts were used in this work in order to compare their wear behaviour and wear mechanisms involved in the grinding process: Samples A are a conventional material previously used, consisting of a 1.2379 high-alloy steel AISI D2 (DIN X155CrVMo12 1), Samples B are steel inserts coated with a thick layer of a metal matrix composite and Samples C are special steels, whose chemical compositions obtained by EPMA (Electron Probe Micro-Analysis) can be seen in Table 1. The process used for coating Samples B was thermal projection. The thickness selected for the coating applied in Sample B was 1.2 mm, as the range of this kind of coatings within this coating process is between 0.5 mm and 2.0 mm. The thickness was selected taking into consideration a balance between abrasion resistance, loads applied on the surface and adhesion of the coating to the substrate, since too thick coatings tend to detach easier from the substrate.

Table 1. Chemical composition of the three samples used in this work, obtained by EPMA.

Reference	C	Si	Mn	Cr	Ni	Cu	Mo	V	W	Fe
A	1.53%	0.30%	0.35%	12.0%	-	-	0.80%	0.80%	-	Balance
B	4.98%	-	-	3.60%	52.1%	-	-	-	Balance	-
C	1.25%	2.65%	0.84%	7.51%	-	0.71%	1.22%	0.98%	-	Balance

2.1.2. Samples Geometric Characterization

The typical geometry of the samples can be observed in Figure 1. As can be seen in that figure, the corners are sharpened, having a greater thickness in that area (excluding samples B), in order to improve the cutting/grinding effect. The sharp edges help to increase grinding performance, contributing as well to drag the raw material from the feeding area to the rotor where the grinding process is effectively carried out.

2.2. Methods

2.2.1. Techniques and Equipment Used in Inserts Characterization

Previously to be mounted in the main tool, the inserts were labelled and weighed in a METTLER, PJ4000 precision balance in order to ease the mass variation analysis. All inserts were also photographed in order to establish eventual morphological differences between the initial and final state of testing and simultaneously help pinpoint the areas where wear phenomena are more evident. In order to facilitate the analyses, one sample was cut using EDM (electrical discharge machining) technique, utilizing ONA AF35 equipment dotted with a 0.33 mm

diameter wire and a 200 mm^2/min cutting speed. In order to verify the chemical composition of the inserts, EPMA equipment JEOL JXA 8500-F was used, allowing access with the desired accuracy to the different contents that compose the inserts material. Furthermore, a Scanning Electron Microscope FEI Quanta 400 FEG ESEM dotted with EDAX Genesis *X*-Ray micro-analysis system was used to characterize the surface morphology of the samples after the previously established work period, helping to identify the wear mechanisms developed on the samples surface as wells as determine the presence or absence of adhered material transferred from the raw material on to the inserts.

Figure 1. Samples geometry.

2.2.2. Hardness Test

Hardness measurements were carried out on the inserts using an EMCO Universal Hardness test equipment, model M4U-025, using diamond Vickers indenter, in order to characterize surface hardness and help predict wear resistance. The selected normal load was 50 N which was kept constant during 30 s, avoiding this way creep phenomenon. This test was performed ten times on different areas of each sample in order to obtain an average value, provided with the required accuracy. These tests were performed according to the ISO 14577-1:2015 [28]. Regarding the geometrical specificity of the samples B, the hardness measurements were performed just in the coating area, which is the main surface exposed to the wear. As the equipment used to measure the hardness does not allow the digital output data, the values were observed in the screen of the equipment and conveyed to an Excel spreadsheet allowing to compute the average values.

2.2.3. Grinding

Grinding operations were carried out with a VECOPLAN, model VAZ 145/250 grinding machine (Figure 2). It is a single shaft shredder with approximately 12" diameter by a 98" wide rotor with bolt-on blades. This rotor has 144 inserts on it. The shredder has an 60" × 98" wide feed opening with a hopper and a hydraulic ram feed and is driven by a 110 kW, 600 V, 895 rpm motor. The established time for the test was 500 working hours. This time was divided into three equal periods, where at the end of each period of time, the cutting inserts would be rotated, allowing three out of the four cutting corners to be tested (one of the corners of the cutting insert was not used due to trials duration). In this period, no special care was taken regarding the machine feeding process, simulating the usual working conditions observed so far.

2.2.4. Tool Holder

The tool holder can support 144 inserts, as depicted partially in Figure 3. To perform the required tests, four inserts of each type used in this work were assembled in the same tool holder area, thus avoiding any different behaviour of the grinding process. The area selected to assemble the inserts was in the middle of the tool holder. As can be seen in previously mentioned figure, the positioning of the inserts was strategically thought to optimize the dragging and grinding effect. The inserts were fixed to the tool holder through a bolting system, allowing easy rotation or replacement. The positioning of each insert allows for two cutting faces and a corner to be exposed to the cork raw material. When a corner is worn, the insert is rotated 90°, exposing the next corner and the two adjacent faces. The grinding effect is produced by pressing the raw cork material against the counter-knives.

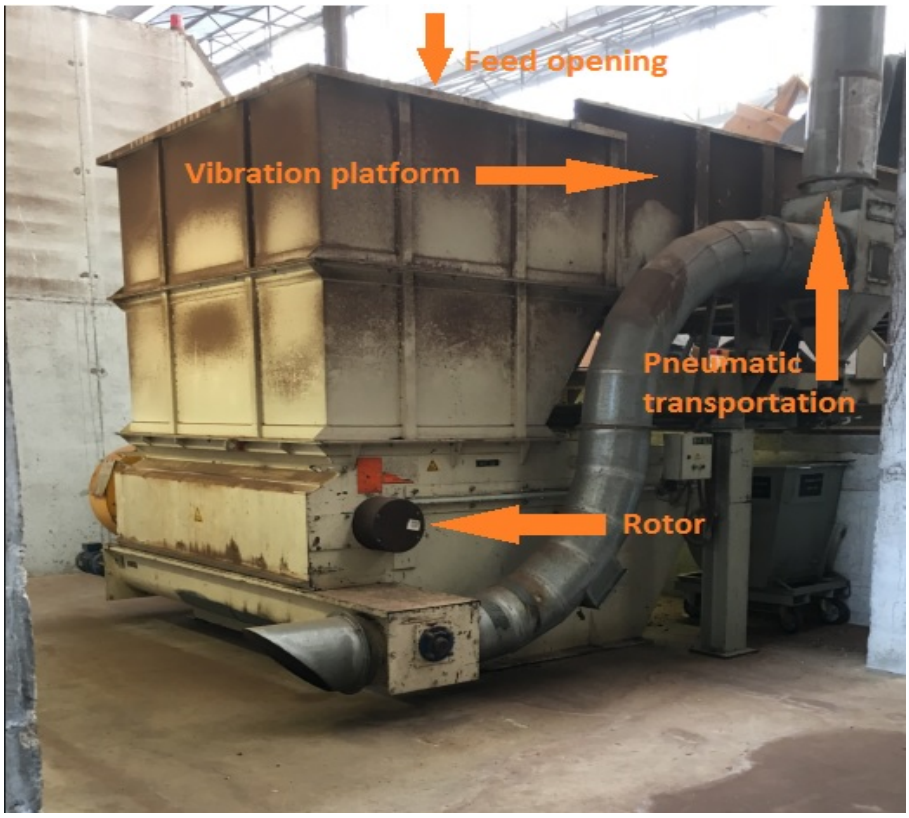

Figure 2. Grinding equipment.

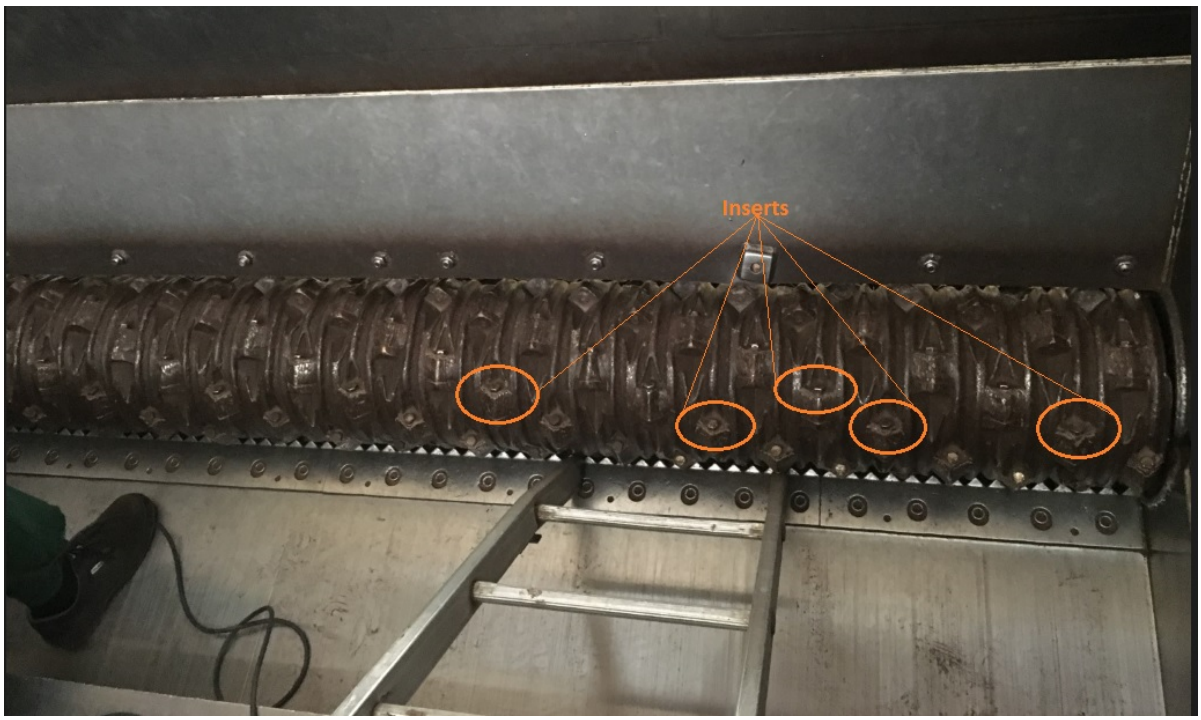

Figure 3. View of the rotor where the inserts are installed.

3. Results and Discussion

3.1. Hardness

The samples were cut in four similar parts, being the inner part subjected to a metallurgical preparation to allow the Vickers tests. The measurements allow the determination of the average value for each sample, which can be seen in Table 2.

Table 2. Results of the hardness test performed in each type of sample.

Sample A	Sample B	Sample C
695.1 ± 21.2 HV5	329.2 ± 16.7 HV5	701.9 ± 28.6 HV5

The results obtained allow conclude that samples B are the softer of the ones tested, despite being coated on the top side of the insert (where the measurements were effectively made). In this case, the indentations enable to realize that there are hard particles in the coating, but they are embedded in a soft matrix. Samples A and C showed higher and very similar values, allowing to expect an identical wear behavior. Dzhemelinskyi et al. analyzing the same material used in sample A of this work, had a hardness result of 550–670 HV5 after heat treatment, which is consistent with the results obtained here given the variation in the composition of each material [29]. Yazıcı, in turn, when analyzing wear on steel cultivation tools, was able to observe that hardness alone is not enough to guarantee tribological performance, requiring a balance between this property and the toughness of the material [30].

3.2. Tool Wear

The inserts used in this study can be seen in Figure 4. Comparing their initial form versus their form after 500 working hours, it is clearly observed that severe wear problems have occurred as well as a significant amount of mass loss. Moreover, it possible to distinguish the three cutting corners that were subjected to the grinding work from the remaining ones, whose show just a small amount of contact with the cork material involved in the process.

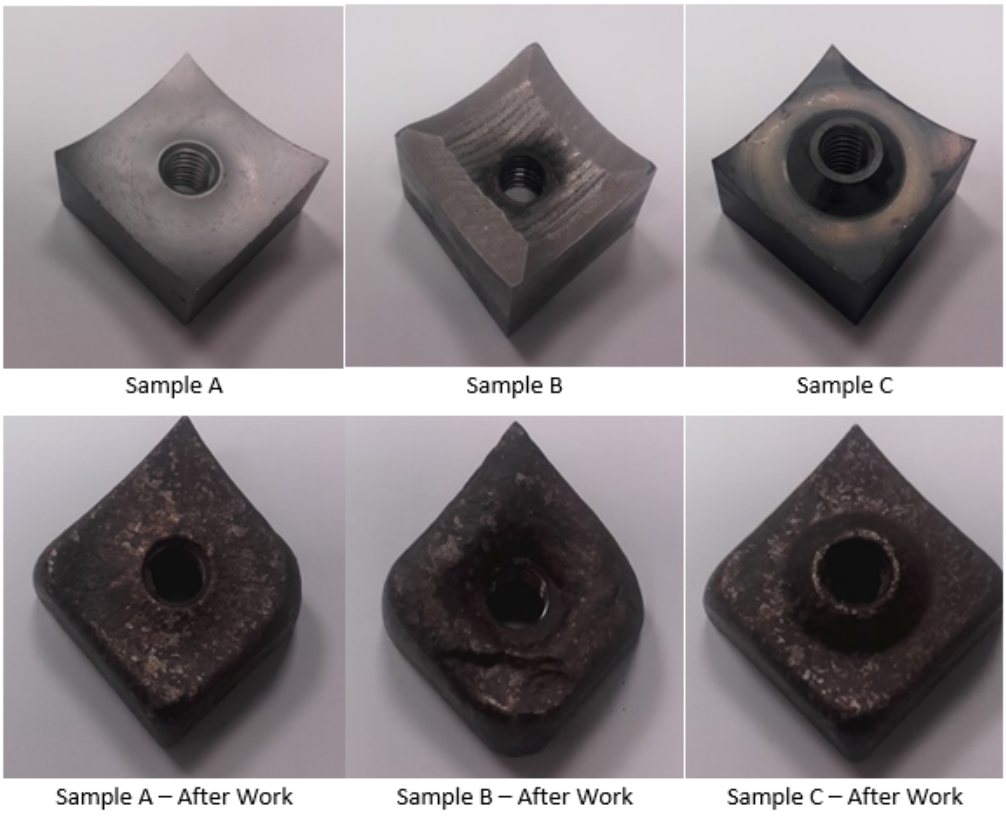

Figure 4. Original and worn samples of each type used in this work.

At the end of the test trials, the inserts were removed from the tool holder for SEM and EDS analyses. The performed analysis aid to better understand the occurred phenomena on the cutting surfaces, as well as the wear mechanism types those occurred on the insert during the grinding. SEM observations were performed on the cutting edges of the tools, where wear is predominant.

The non-worked corner of each sample was taken as a reference for the comparing study. In Figure 5 the non-worked corner of Sample A can be observed, showing an almost-perfect square shape. It must be considered that, despite being a non-worked corner, it was exposed to randomly passing cork resulting from the working area (adjacent corners). The slightly darker areas observed in Figure 5b correspond to a thin layer of cork adhered to the surface. This figure also allows to observe the sample's main chemical contents behind that dark area (Fe, Si, Cr, etc.), as well as C and O correspondent to the cork (Zone 1). On the other hand, in the spectrum relative to

Zone 2, it is possible to observe a strong peak of Si accompanied by other smaller peaks of other minerals such as Mg and Ca, which have originated from sand and dirt contaminations that are introduced into the grinder mixed with cork raw material (a negative side effect resulting from the cork extraction process). Regarding the darker area shown in Zone 3, it is possible to see that there is a strong presence of C and O indicating a large incidence of cork in this area, as well as a light presence of the other previously referred elements corresponding to the sample composition.

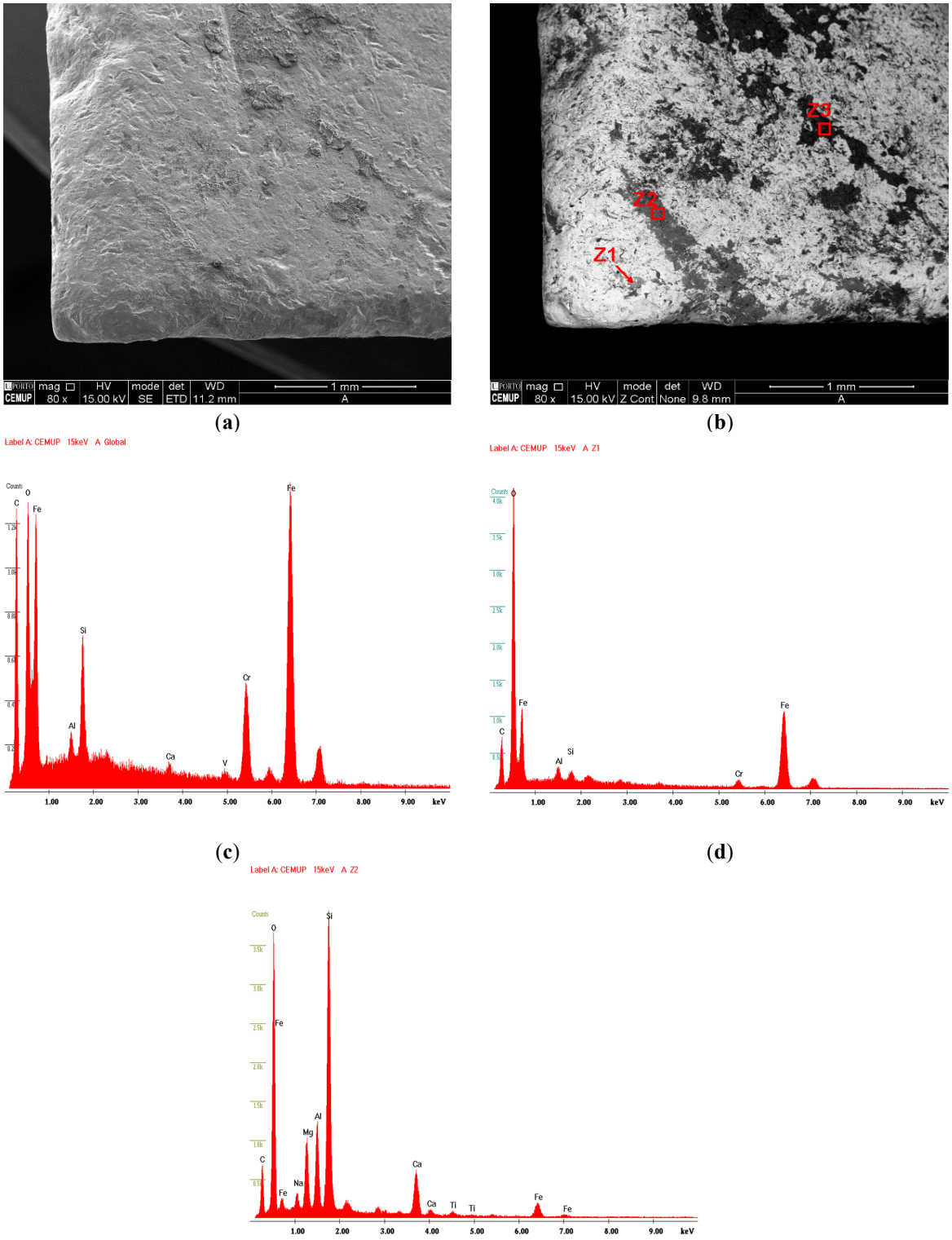

Figure 5. Pictures of the non-worked A sample and corresponding EDS spectra in a generic aspect and detailed areas: (**a**) non-worked corner of Sample A; (**b**) thin layer of cork adhered to the surface; (**c**) zone 1; (**d**) zone 2; (**e**) zone 3.

Figure 6 depicts the worked sample A, showing strong wear. As can be seen, an almost-perfect square shaped corner gave rise to round corner geometry. A detailed view of this worn surface can be seen on the right-hand side of the same figure. This figure also illustrates that the sample surface was polished, losing its roughness peaks, corresponding to a loss of mass. In this case, due to the permanent and intensive flow of cork over the surface, there are no dark areas corresponding to cork adhesion. The abrasion produced by sand particles is responsible for some clear, but rare, scratches. This leads to changes in the geometry of the insert based on gradual wear, which can also lead to a reduction in cutting efficiency and accelerated tool wear. Therefore, the selection of material and cutting tool grade is an important factor to consider when planning a successful operation.

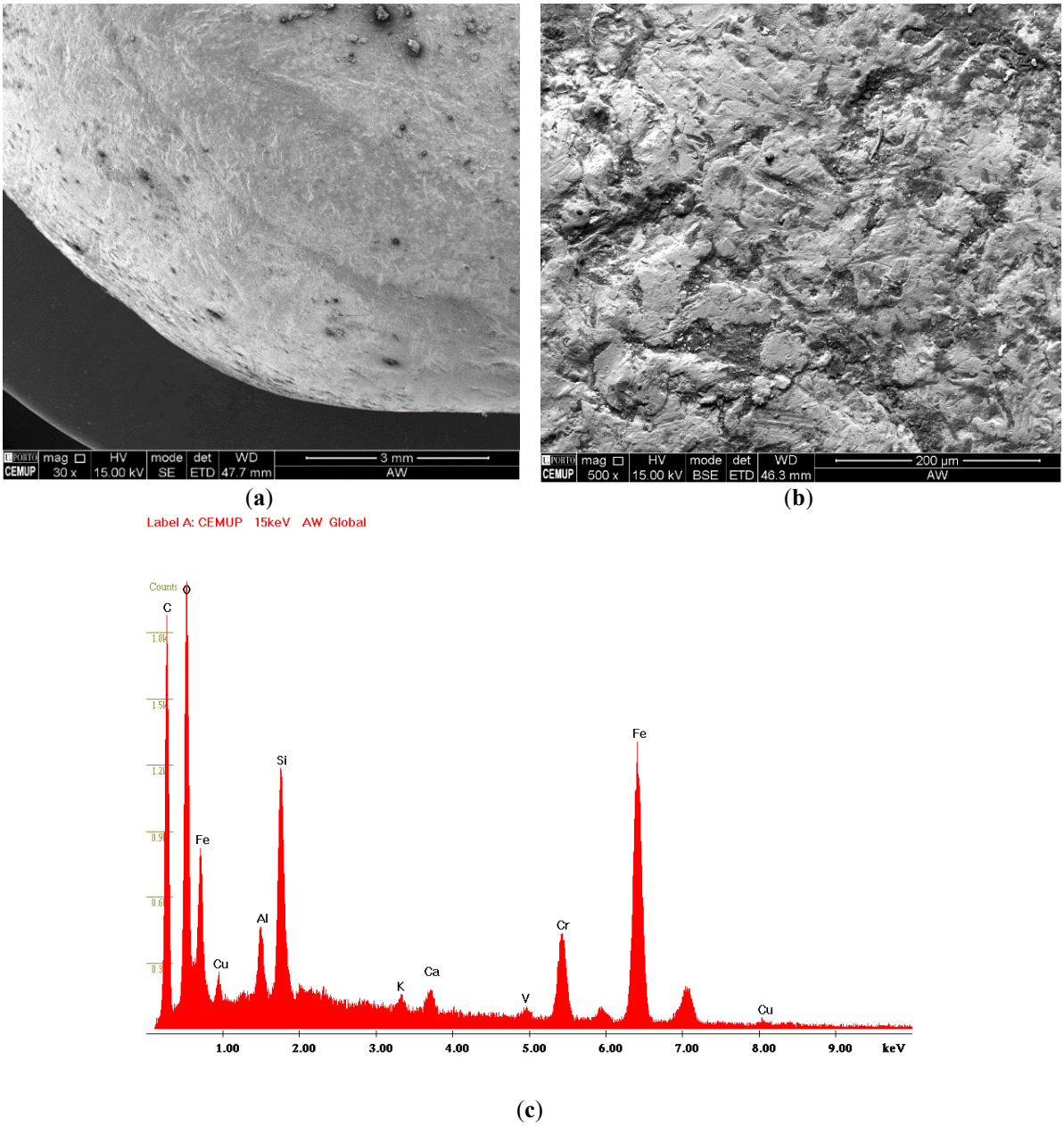

Figure 6. Pictures about the worked A sample and corresponding EDS: (**a**) worked sample A; (**b**) strong wear; and (**c**) corresponding EDS.

Figure 7 shows the non-worked corner of Sample B, letting to also observe an almost-perfect square shape. As in the former case, it must be taken into account that, despite being a non-worked corner, it was exposed randomly to cork routed from the effective working area (adjacent corners). Three different areas were analyzed in order to confirm the coating composition and determine the different phases present on each surface. Regardless of the different observable shades viewed in Figure 7, W is predominant throughout all of the chemical spectrum, being possible also to observe some small peaks of other elements such as Cr, Ni and Si, corresponding to the main constituents of the thick surface coating used on this sample.

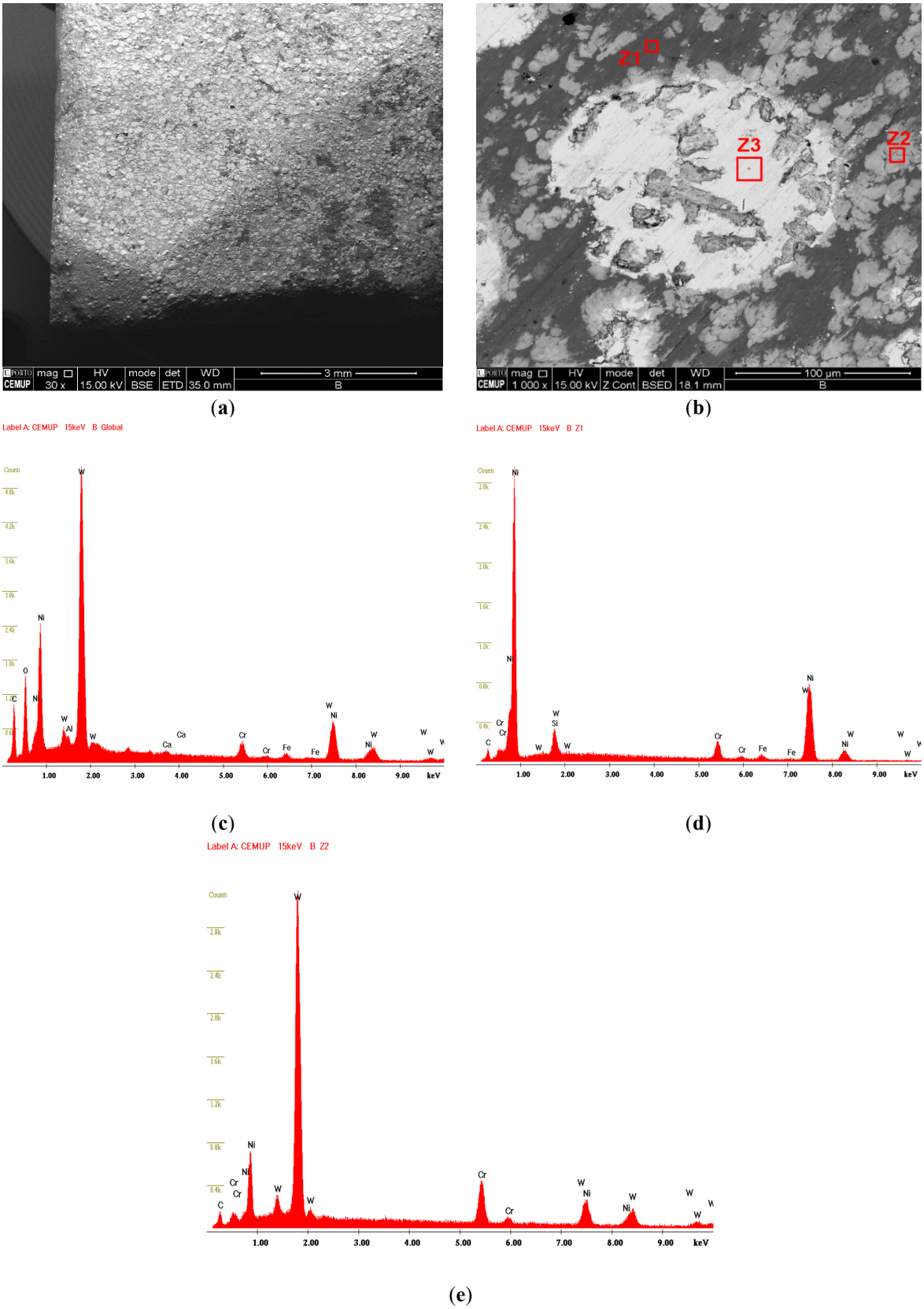

Figure 7. Pictures of the non-worked B sample and corresponding EDS spectra in a generic aspect and detailed areas: (**a**) non-worked corner of Sample B; (**b**) zones to analyze the EDS; (**c**) zone 1; (**d**) zone 2; (**e**) zone 3.

In Figure 8 it is possible to observe a detailed image regarding one of the worn corners as well as a detail image of the surface. The different shades shown correspond to different products adhered to the surface. White areas corresponding to Z1 are related to W spheres that tend to remain on the surface, whereas the darker areas labelled as Z2 show a strong peak of Si. Effectively, the existence of Si in some areas can be attributed once again to the introduction of sand contaminants from the cork raw material, caused by a careless cutting process of the

tree skin and subsequent necessary transportation and logistics operations. As an example, the tree skin is cut and deposited on the ground close to the tree, thereafter bulldozers collect the tree skin portions from the soil and simultaneously collect dirt and sand alongside the raw material, which shall remain together until reaching the grinding machine's initial container. This surface phenomenon is new relatively to Sample A, which showed a different behavior. Indeed, the presence of sand in sample B is only possible due to presence of a coating composed of W hard spheres embedded in a Ni soft matrix, which allows accommodate the hard sand particles. Effectively, the sand particles do not remain on the surface of sample A because there is a lower hard difference between the sand and the heat-treated steel surface of sample A. On the other hand, light dark areas corresponding to Z3 are related to the Ni matrix, showing clear peaks of this element. When observing with attention this surface, it is possible to state that the Ni matrix is easily consumed relative to the W spheres, these being highlighted relatively to the Ni matrix. However, even though these hard spheres show signs of abrasion wear, it is possible to observe a polished surface.

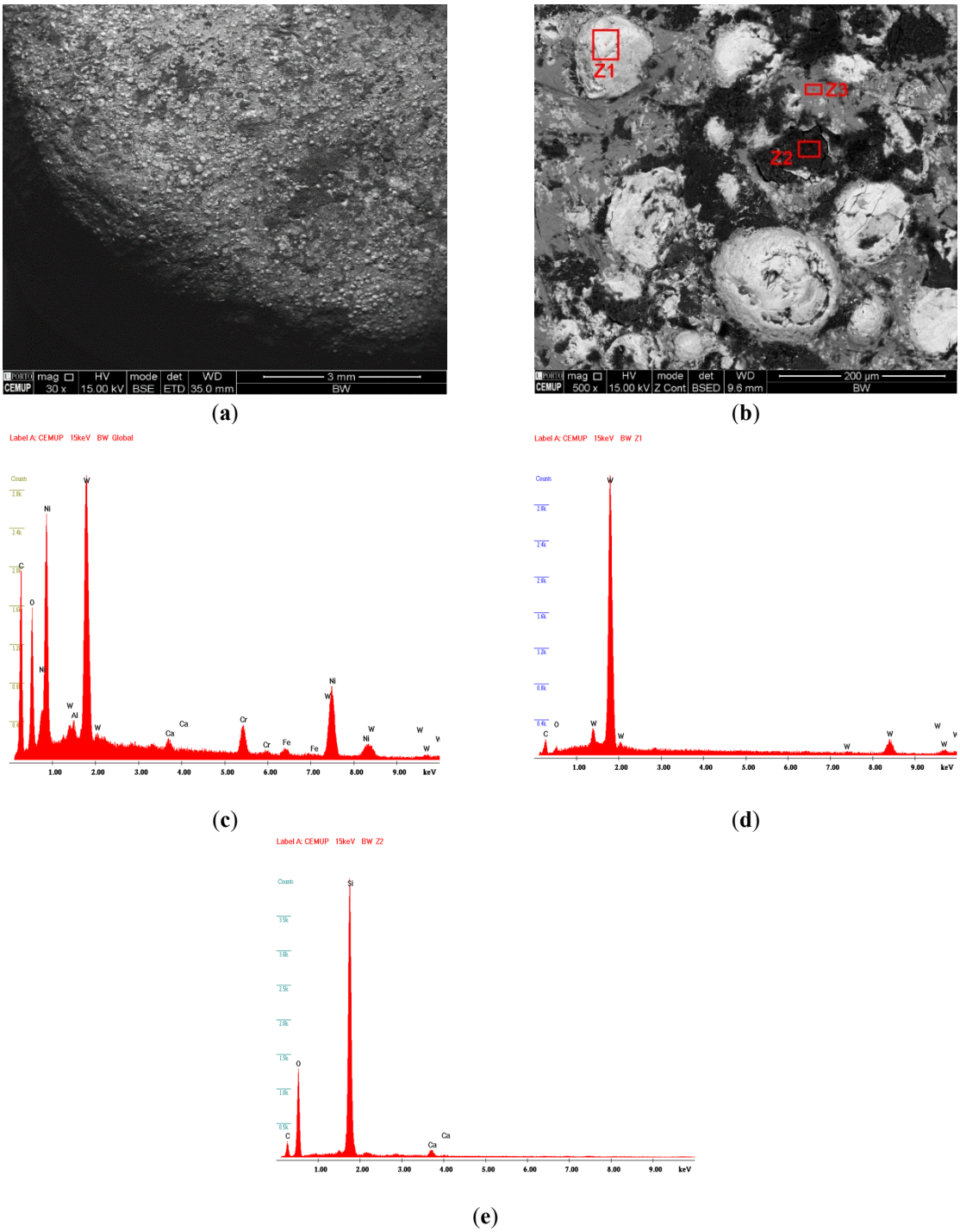

Figure 8. Pictures of the worked B sample and corresponding EDS spectra in a generic aspect and detailed areas (**a**) worked B sample; (**b**) zones to analyze the EDS; (**c**) zone 1; (**d**) zone 2; (**e**) zone 3.

In Figure 9 it is possible to observe the non-worked corner relatively to Sample C, showing again an almost-perfect square shape. The EDS spectrum shown in this figure clearly depicts the composition of the sample described in Table 1. The surface morphology of sample C can be perfectly compared to the remaining ones, mainly sample A.

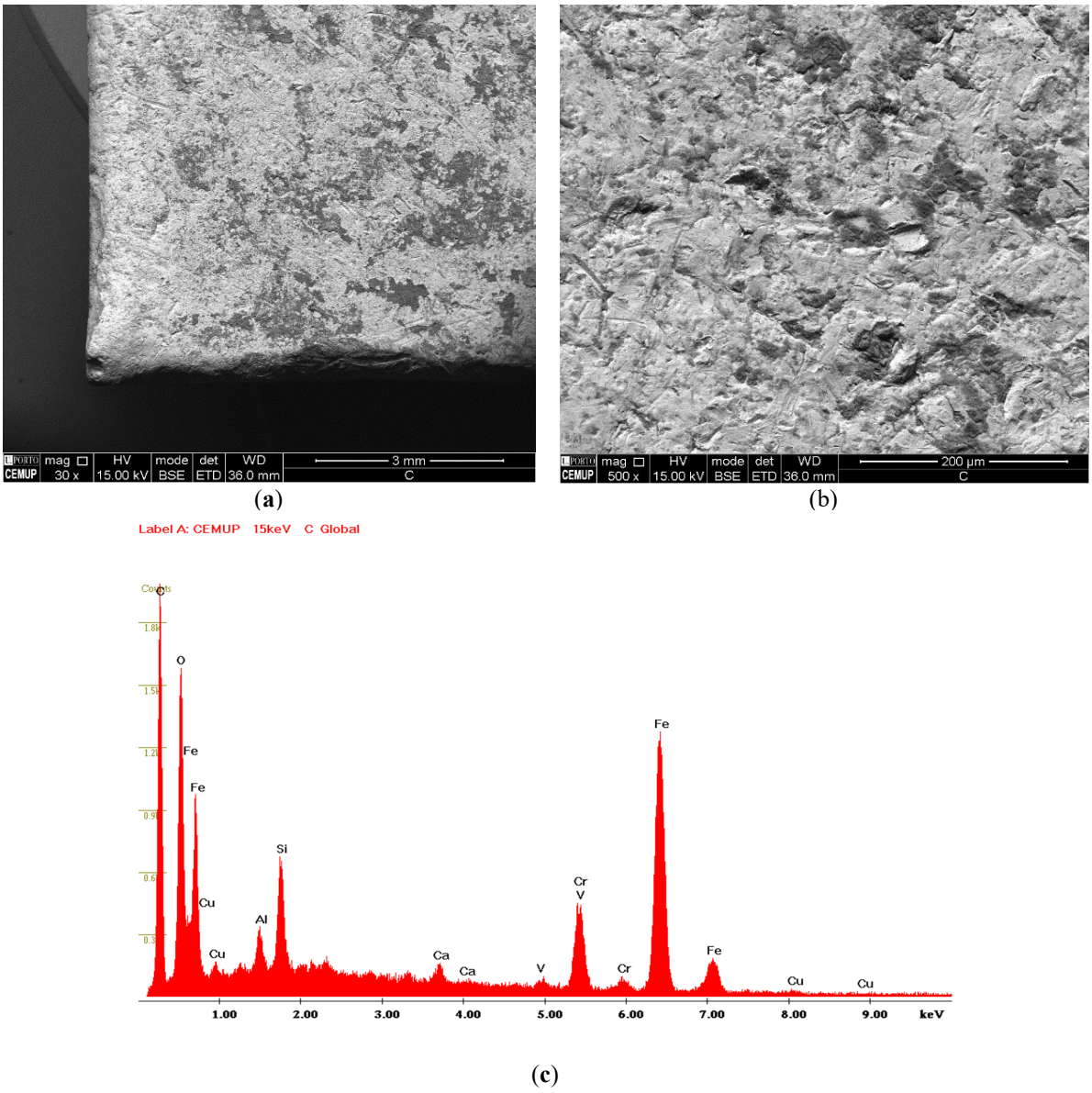

Figure 9. Pictures of the non-worked C sample and corresponding EDS spectra in a generic aspect and detailed areas (**a**) non-worked C sample; (**b**) expansion of the area and further details; and (**c**) EDS.

Figure 10 depicts the worked area of sample C, showing strong wear. As can be seen, the almost-perfect square shape of the corner gave rise to a round corner shape. However, when comparing the detailed worn surface of sample C with a worn surface from sample A, it can be observed that sample A shows a more polished aspect, being expected to lose a higher mass than in sample C. Indeed, the worn surface of sample C presented in Figure 10 shows the presence of sharp structures, remaining like the one viewed in the non-worked surface, (mass loss analysis will further confirm this phenomena). When comparing the hardness values between samples A and C, the difference is almost irrelevant. However, the behavior of sample C shows to be better than sample A and much more effective than the coating used in sample B. As can also be observed, there are no deposits of raw material on the surface as well as any clear marks of erosion or abrasion produced by sand or dirt particles. Thus, regardless of the rounded shape shown in Figure 10a, the surface shows a more preserved aspect with some deep marks induced by strange elements introduced in the process, such as stones, sand and other non-expected hard elements.

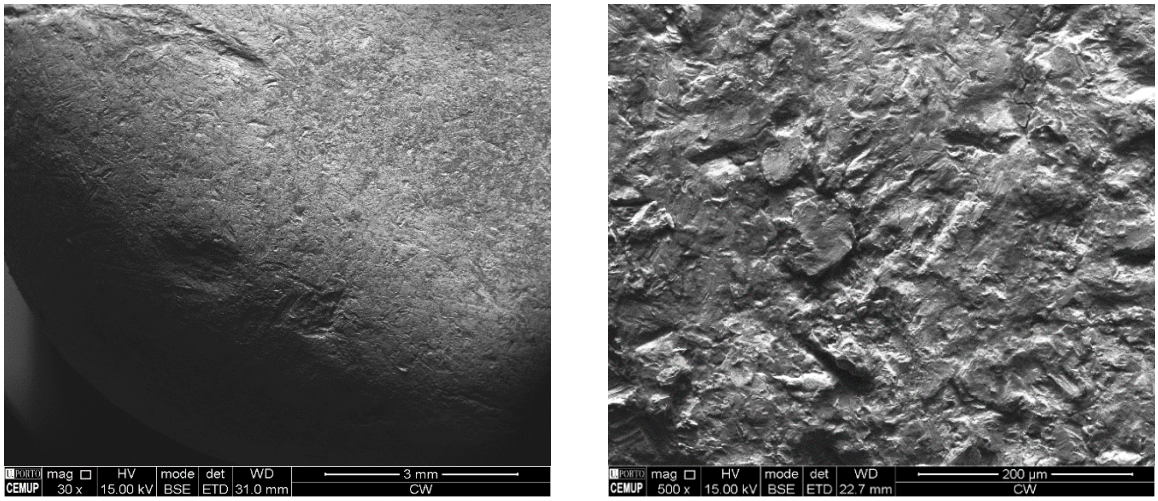

(**a**) (**b**)

Figure 10. Pictures of the worked C sample (**a**) worked C sample and (**b**) wear.

The insert hardness significantly influences wear; specifically, the wear rate rises with any small decrease in sample hardness, consistent with existing studies, as for example found in [31–34]. As in the study by [35], the softer material suffered more significant wear. According to the authors, reducing abrasive wear is essential for reducing economic losses, especially in the mining industry. When analyzing the wear of cemented carbides with tungsten carbide grains used in drill bit inserts, Toller-Nordstrom et al. found that wear progresses through material fracture [36]. In turn, Grejtak et al. evaluated the wear of crusher cutters and found that their durability can be substantially improved by using more wear-resistant tool materials; in this case, iron performed best in this regard [37]. To compare the wear resistance of drill bit inserts, Saai et al. evaluated several materials with different grain sizes and found that microstructure is the most important factor in wear behavior [38]. Thus, as seen in this work, each type of material behaves differently when subjected to wear.

3.3. Analisys of Mass Loss

In order to determine the total wear suffered by the different inserts and as previously referred, the inserts were weighted using a precision scale, allowing the comparison between the initial and final weight of the insert samples. From Figure 11 is possible to observe that sample A presented a cumulative mass loss (for all 4 samples) of 30.67 g, which represents an average of 7.67% for this sample. Attending that just three corners were used in this work, the values were standardized, being extrapolated to four corners.

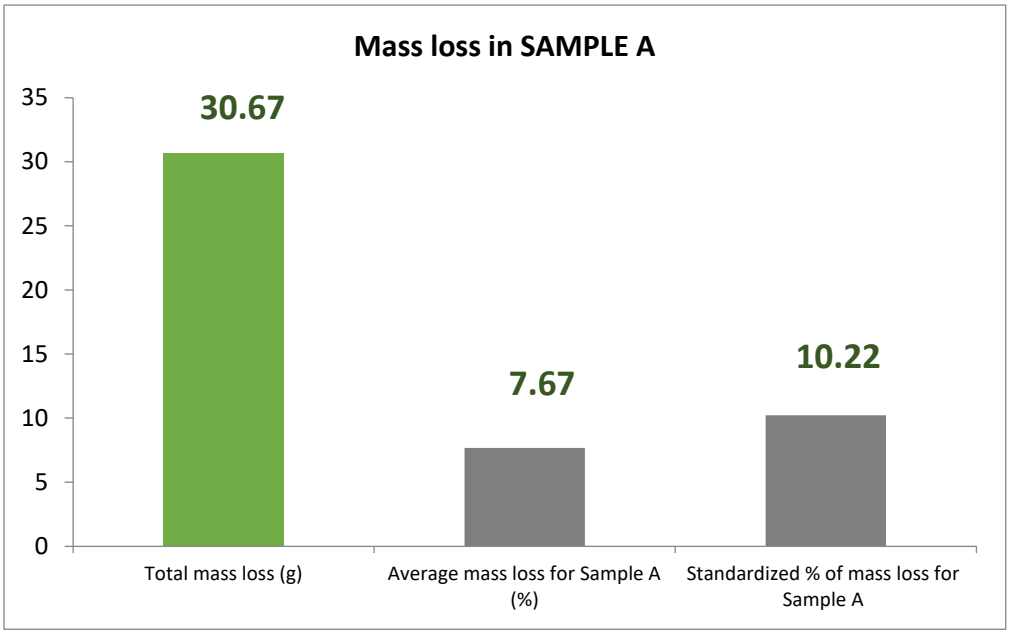

Figure 11. Sample A mass loss.

By measuring the height of each sample, it became possible to understand how wear occurred along the sample's edges. Viewing Figure 12 it is possible to observe that despite samples A having presented the biggest height loss (46.91 mm for this set of samples), these samples do not present the highest mass loss. This analysis allows understand that these samples are stiff enough to resist wear, but their corners tend to be easily abraded, showing a slightly poorer toughness and abrasion resistance.

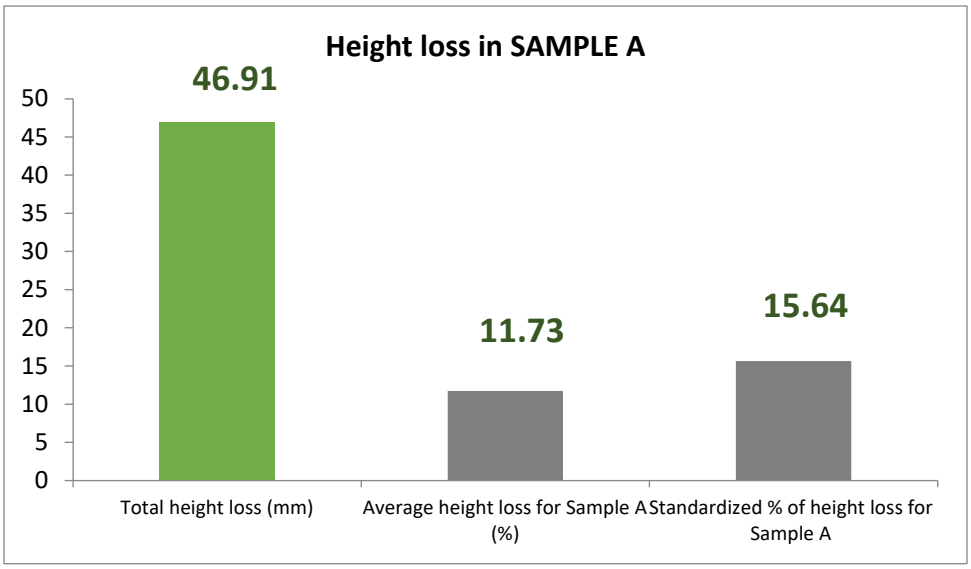

Figure 12. Height Loss of Sample A.

Regarding samples B, it is possible to observe in Figure 13 that the total mass loss was 79.88 g which represents the highest lost from all of the sample groups. The average of mass loss was 19.97% which is more than the double when compared to the results of samples A and C. This mass loss indicates that the material is too soft for grinding raw cork material, showing poor abrasion resistance.

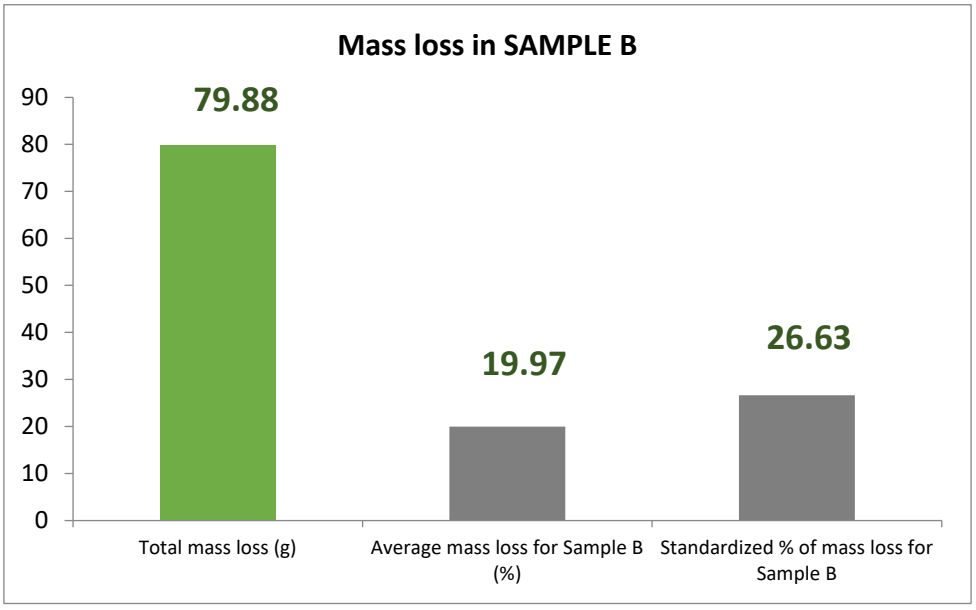

Figure 13. Sample B mass loss.

Despite the highest mass loss shown by samples B, these were not the ones where the height loss was greater. In fact, samples B were the ones where the height loss was the lowest. From Figure 14 it is possible to observe that these samples lost 37.57 mm in total, which refers to 9.39% of average height lost from the four B samples tested. Regarding the composition of the coating used in these samples, it is possible to state that they are losing mass due to the abrasion of the Ni matrix, however, W hard particles are remaining on the surface until the critical embedded surface isn't strong enough to secure their position. This phenomenon positively influenced the height measurements.

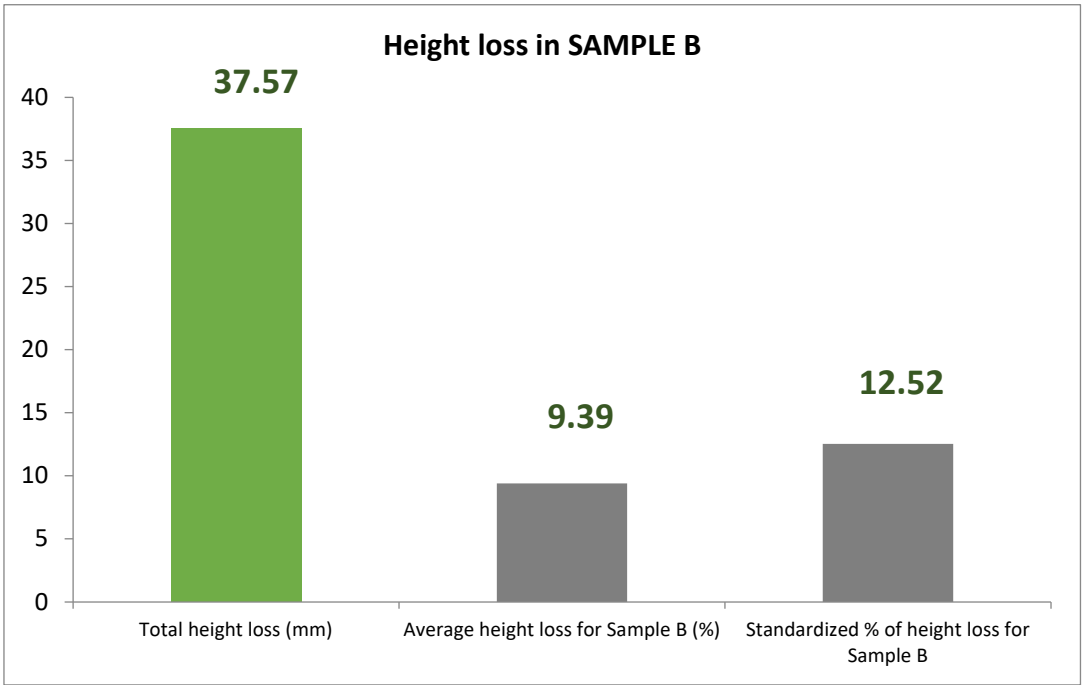

Figure 14. Sample B height loss.

Samples C were the samples which presented the less mass lost, just 27.85 g as observer in Figure 15. The composition of the C samples shows a better abrasion and erosion resistance when grinding cork raw material (including unexpected contents), allowing a longer service time than other inserts as these lost much less mass during the established test time.

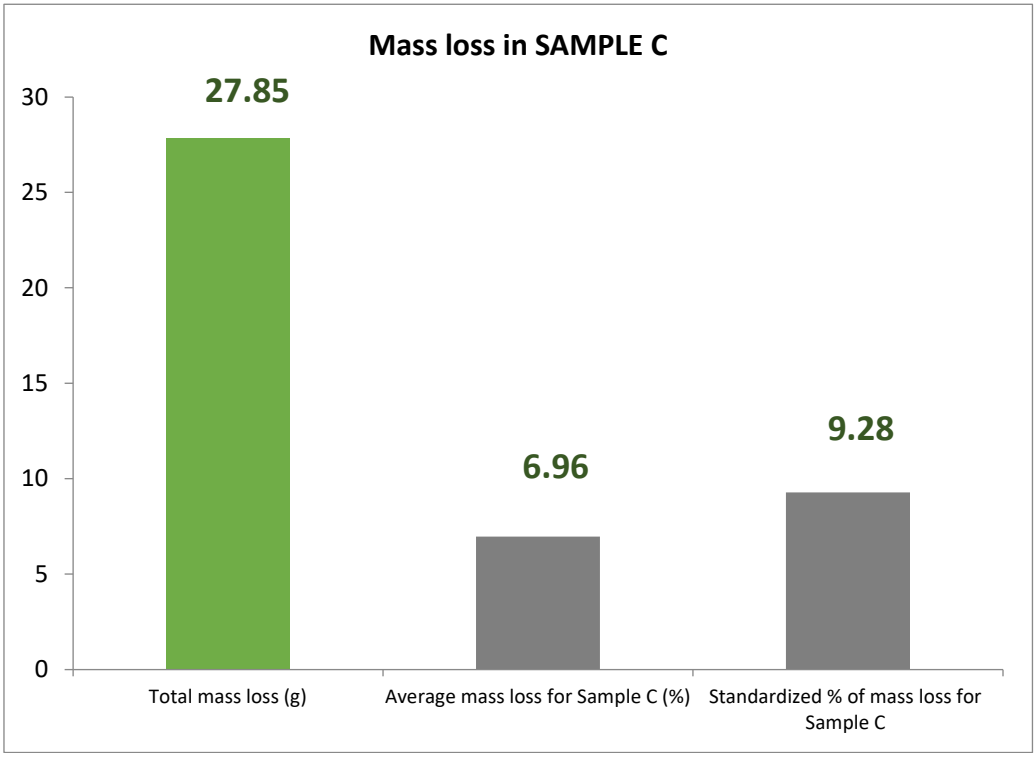

Figure 15. Sample C mass loss.

Concerning the height loss seen in samples C, it is possible to realize from Figure 16 that these samples presented a total height loss of 38.51 mm, with an average value of 9.63% per sample.

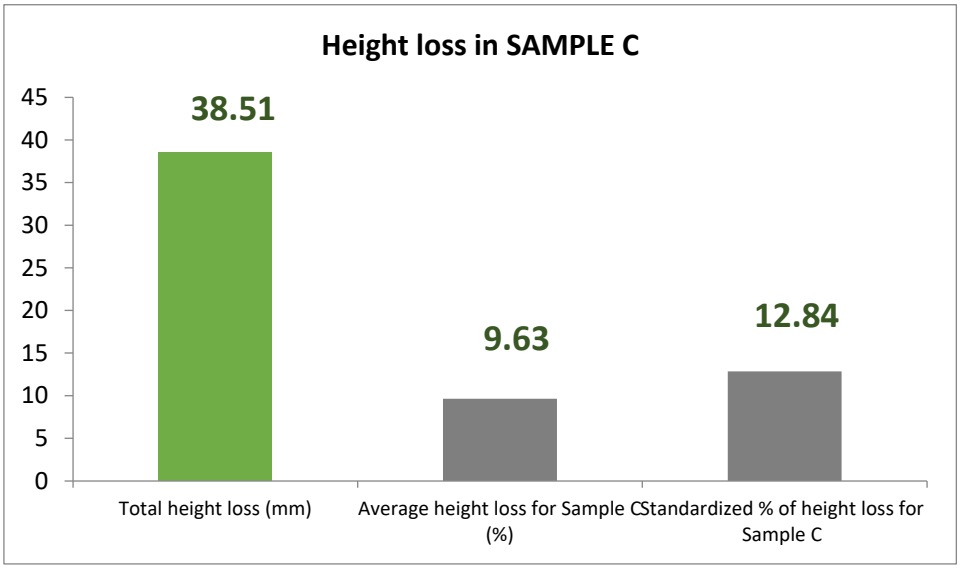

Figure 16. Sample C height loss.

This analysis allows to understand that samples C presented a height loss very similar to the lowest value registered (achieved by samples B), letting to affirm that they present the best compromise between mass loss and height loss, showing the best behaviour in this comparative work. According to [39], the use of a narrower particle size distribution leads to less volume loss.

Based on these results, the inserts from sample group C were those who presented the best wear resistance, showing a good compromise between hardness and toughness. The sharp edge geometry is very useful to increase the cutting performance throughout the first working stages of each sample's corner, but they lose cutting efficiency due to the fast wear felt seen in all samples in this specific area of the cutting inserts.

It is not easy to find a coating that is able to deal with the required properties set by these cutting systems, mainly when unexpected objects are introduced in the cutting area, namely stones and sand, which highly interfere with the inserts lifespan in a drastic manner.

The performance and ultimate service life of tool inserts are critically determined by the interaction between the insert material and the working environment. In grinding processes, tool wear is typically the result of the synergistic action of several distinct mechanisms, often compounded by the presence of hard contaminants, high temperatures, and cyclical stresses. Understanding these fundamental mechanisms is paramount for selecting the optimal material and developing effective mitigation strategies. Table 3 summarizes the most significant wear mechanisms encountered in the service of metallic inserts in high-stress applications. The table outlines the physical processes, characteristic morphological features, and primary relevance of each mechanism.

Table 3. Summary of major wear mechanisms, their characteristics, and relevance to metallic inserts in grinding applications.

Wear Mechanism	Description/Propagation	Typical Appearance on Inserts	Relevance to Grinding
Abrasive Wear	Material removal by hard particles (contaminants) scratching or ploughing the surface. Propagates via groove formation and micro-cutting.	Grooves, scratches, parallel marks.	Highly relevant due to contaminants (silica, minerals) in cork.
Adhesive Wear	Transfer of material fragments between the two contact surfaces (insert and cork/contaminant). Propagates through micro-welding and shearing.	Material transfer, welding spots, tearing.	Relevant at high contact temperatures/pressures.
Fatigue Wear	Surface or sub-surface crack initiation and propagation due to cyclical thermal/mechanical stress. Leads to material loss (pitting/spalling).	Micro-cracks, pitting, spalling.	Relevant due to intermittent or cyclical loading during cutting.
Fracture/Chipping	Rapid material removal due to high local stress concentration. Propagates via brittle crack growth.	Large fragments loss, chipping at the cutting edge.	Relevant if the material's toughness is insufficient for the impact loading.

4. Conclusions

Regarding the results obtained and described in the previous sections, it is possible to make a comparable summary about them, drawing the following conclusions:

- The main wear mechanism affecting the inserts in cork grinding process is abrasion. However, erosion can also occur due to material projected into the grinder. Abrasion is produced by cork material but the main abrasive materials in the process are sand and dirt in general (earth, for example) those are fed together with the cork skin extracted from the tree. This is hard to prevent without a separation system using vibration devices and filtering processes;
- Coating used in samples B are not suitable for this kind of application because, even though they present hard W spheres, the insert's matrix is not hard enough to accommodate the erosion and abrasion wear promoted by sand and dirt fed alongside with the raw material;
- Samples B showed the lowest height lost values because of the W spheres that remain on the worn surface, masking the mass lost values. Moreover, regardless of the lowest height loss presented by these samples, the cutting effect was lost, being the height supported by rounded W particles embedded in the Ni matrix;
- Samples A and C, being different in terms of compositions, shows similar hardness values but different wear performance;
- Samples A is more suitable to accommodate debris in their surfaces, namely cork layers with different thicknesses;
- Samples C show the best wear behaviour, presenting the lowest mass lost values (samples A and B) and very close values to the best height lost values presented by samples B;
- Hardness is the property that seems to be essential to ensure a good wear behaviour, however, extremely hard surfaces can lead to insert failure due to low toughness, which plays an important role when inserts collide with hard foreign objects;
- Composition of Sample C is the most wear-resistant for this kind of application, regarding the three different samples used in this work, allowing the longest lifespan in this set of samples. The composition/microstructure of Sample C suggests that it will have better edge retention and abrasion resistance, while its toughness and fracture toughness, although not directly measured, did not show catastrophic failure during the 500-h test.

Thus, abrasion seems to be the main wear mechanism affecting the surface of the inserts, being that samples C have the most appropriate composition to deal with the wear phenomena induced by the cork raw material and its inevitable contaminants. Further studies should be done in order to improve the surface hardness, trying to keep the toughness values in an acceptable range to accommodate the eventual introduction of foreign materials in the process. Thick coatings can be considered in further studies but need to be carefully designed in order to increase their homogeneity and improve the wear behaviour resistance, without compromising the surface stiffness and toughness. Future research should focus on implementing and testing novel engineering interventions to significantly enhance their performance and lifespan. A key area of exploration includes surface engineering techniques such as laser surface texturing. This technique offers a promising approach to modify the surface topography, potentially improving lubrication retention and reducing the coefficient of friction, thereby mitigating abrasive wear and micro-pitting. Furthermore, exploring next-generation multilayer coatings or the application of specialized thermal treatments could also lead to optimized wear resistance, particularly for the high-alloy steel and the metal matrix composite inserts, offering a path toward an optimized and durable grinding solution.

Author Contributions

E.T.O. and N.P.V.S: conceptualization; A.B., G.P. and I.I.: methodology; E.T.O. and N.P.V.S.: data curation, visualization; A.B.: writing—original draft preparation; E.T.O. and N.P.V.S.: investigation; G.P.: supervision; A.B. and G.P.: validation; I.I.: writing—reviewing and editing. All authors have read and agreed to the published version of the manuscript.

Funding

The work is developed under the "DRIVOLUTION—Transition to the factory of the future", with the reference DRIVOLUTION C644913740-00000022 research project, supported by European Structural and Investments Funds with the "Portugal2020" program scope.

Institutional Review Board Statement

Not applicable.

Informed Consent Statement

Not applicable.

Data Availability Statement

Not applicable.

Conflicts of Interest

The authors declare no conflict of interest. Given the role as Editorial Board Member, Iván Iglesias had no involvement in the peer review of this paper and had no access to information regarding its peer-review process. Full responsibility for the editorial process of this paper was delegated to another editor of the journal.

Use of AI and AI-Assisted Technologies

No AI tools were utilized for this paper.

References

1. Gil, L. Cork Composites: A Review. *Materials* **2009**, *2*, 776–789. https://doi.org/10.3390/ma2030776.
2. Gil, L. New Cork-Based Materials and Applications. *Materials* **2015**, *8*, 625–637. https://doi.org/10.3390/ma8020625.
3. Gil, L. Cork: A strategic material. *Front. Chem.* **2014**, *2*, 16. https://doi.org/10.3389/fchem.2014.00016.
4. Santos, T.; Amaral, J.S.; Amaral, V.S.; et al. In-plane thermal anisotropy of natural cork and its variability. *Measurement* **2025**, *242*, 116062. https://doi.org/10.1016/j.measurement.2024.116062.
5. Lakreb, N.; Şen, U.; Toussaint, E.; et al. Physical properties and thermal conductivity of cork-based sandwich panels for building insulation. *Constr. Build. Mater.* **2023**, *368*, 130420. https://doi.org/10.1016/j.conbuildmat.2023.130420.
6. Gerometta, M.; Gabrion, X.; Lagorce, A.; et al. Towards better understanding of the strain–stress curve of cork: A structure–mechanical properties approach. *Mater. Des.* **2023**, *235*, 112376. https://doi.org/10.1016/j.matdes.2023.112376.
7. Paulo, J.A.; Santos, D.I. Virgin cork colour and porosity as predictors for secondary cork industrial quality. *Ind. Crops Prod.* **2023**, *205*, 117513. https://doi.org/10.1016/j.indcrop.2023.117513.
8. Anjos, O.; Pereira, H.; Rosa, M.E. Effect of quality, porosity and density on the compression properties of cork. *Holz Als Roh-Und Werkst.* **2008**, *66*, 295–301. https://doi.org/10.1007/s00107-008-0248-2.
9. Silva, S.P.; Sabino, M.A.; Fernandes, E.M.; et al. Cork: Properties, capabilities and applications. *Int. Mater. Rev.* **2005**, *50*, 345–365. https://doi.org/10.1179/174328005X41168.
10. Oliveira, V.; Pereira, H. Cork and Cork Stoppers: Quality and Performance. In *Chemistry and Biochemistry of Winemaking, Wine Stabilization and Aging*; IntechOpen: London, UK, 2021. https://doi.org/10.5772/intechopen.92561.
11. Fonseca, A.P.; Adame, C.F.; Teodoro, O.M.N.D. The role of coatings on the sealing of cork stoppers. *J. Food Eng.* **2024**, *378*, 112114. https://doi.org/10.1016/j.jfoodeng.2024.112114.
12. Suffo, M.; Pérez-Muñoz, C.; Alba, G.; et al. An Innovative Polypropylene/Waste Cork Composite Material for Spirit and Wine Stopper Caps. *Appl. Sci.* **2024**, *14*, 3014. https://doi.org/10.3390/app14073014.
13. Castro, O.; Silva, J.M.; Devezas, T.; et al. Cork agglomerates as an ideal core material in lightweight structures. *Mater. Des.* **2010**, *31*, 425–432. https://doi.org/10.1016/j.matdes.2009.05.039.
14. Gil, L. Cork. In *Materials for Construction and Civil Engineering*; Springer International Publishing: Cham, Switzerland, 2015; pp. 585–627. https://doi.org/10.1007/978-3-319-08236-3_13.
15. Pinto, C.; Cravo, S.; Mota, S.; et al. Cork by-products as a sustainable source of potential antioxidants. *Sustain. Chem. Pharm.* **2023**, *36*, 101252. https://doi.org/10.1016/j.scp.2023.101252.
16. Reculusa, S.; Trinquecoste, M.; Dariol, L.; et al. Formation of low-density carbon materials through thermal degradation of a cork-based composite. *Carbon* **2006**, *44*, 1316–1320. https://doi.org/10.1016/j.carbon.2005.12.051.
17. Pintor, A.M.A.; Ferreira, C.I.A.; Pereira, J.C.; et al. Use of cork powder and granules for the adsorption of pollutants: A review. *Water Res.* **2012**, *46*, 3152–3166. https://doi.org/10.1016/j.watres.2012.03.048.
18. Saadallah, Y.; Zemour, I.; Boulemnakher, F. Experimental investigation of mechanical behavior of agglomerated cork. *Mater. Des. Process. Commun.* **2020**, *2*, e123.
19. Vaz, M.F.; Fortes, M.A. Friction properties of cork. *J. Mater. Sci.* **1998**, *33*, 2087–2093. https://doi.org/10.1023/A:1004315118535.
20. Martínez-Martínez, D.; Tiss, B.; Glanzmann, L.N.; et al. Protective films on complex substrates of thermoplastic and cellular elastomers: Prospective applications to rubber, nylon and cork. *Surf. Coat. Technol.* **2022**, *442*, 128405. https://doi.org/10.1016/j.surfcoat.2022.128405.

21. Fang, X.D.; Yao, Y.; Arndt, G. Monitoring groove wear development in cutting tools via stochastic modelling of three-dimensional vibrations. *Wear* **1991**, *151*, 143–156. https://doi.org/10.1016/0043-1648(91)90354-W.
22. Liu, Z.Q.; Ai, X.; Zhang, H.; et al. Wear patterns and mechanisms of cutting tools in high-speed face milling. *J. Mater. Process. Technol.* **2002**, *129*, 222–226. https://doi.org/10.1016/S0924-0136(02)00605-2.
23. Shen, Z.; Lu, L.; Sun, J.; et al. Wear patterns and wear mechanisms of cutting tools used during the manufacturing of chopped carbon fiber. *Int. J. Mach. Tools Manuf.* **2015**, *97*, 1–10. https://doi.org/10.1016/j.ijmachtools.2015.06.008.
24. Yan, G.; Yue, W.; Meng, D.; et al. Wear performances and mechanisms of ultrahard polycrystalline diamond composite material grinded against granite. *Int. J. Refract. Met. Hard Mater.* **2016**, *54*, 46–53. https://doi.org/10.1016/j.ijrmhm.2015.07.014.
25. Fan, S.; Zhang, L.; Cheng, L.; et al. Wear mechanisms of the C/SiC brake materials. *Tribol. Int.* **2011**, *44*, 25–28. https://doi.org/10.1016/j.triboint.2010.09.003.
26. Maranho, O.; Rodrigues, D.; Boccalini, M.; et al. Mass loss and wear mechanisms of HVOF-sprayed multi-component white cast iron coatings. *Wear* **2012**, *274*, 162–167. https://doi.org/10.1016/j.wear.2011.08.024.
27. Behera, B.C.; Ghosh, S.; Rao, P.V. Wear behavior of PVD TiN coated carbide inserts during machining of Nimonic 90 and Ti6Al4V superalloys under dry and MQL conditions. *Ceram. Int.* **2016**, *42*, 14873–14885. https://doi.org/10.1016/j.ceramint.2016.06.124.
28. *ISO 14577-1:2015*; Metallic Materials—Instrumented Indentation Test for Hardness and Materials Parameters. Part 1: Test Method. ISO: Geneva, Switzerland, 2015.
29. Dzhemelinskyi, V.; Hruska, M.; Mordyuk, B.; et al. Surface Hardness Improvement of AISI D2 Tool Steel by Laser Transformation Hardening Process Using High-Power Disk Laser. In *Advances in Design, Simulation and Manufacturing VII*; Springer: Cham, Switzerland, 2024; pp. 178–187. https://doi.org/10.1007/978-3-031-61797-3_15.
30. Yazıcı, A. Wear on steel tillage tools: A review of material, soil and dynamic conditions. *Soil Tillage Res.* **2024**, *242*, 106161. https://doi.org/10.1016/j.still.2024.106161.
31. Luyckx, S.; Sacks, N.; Love, A. Increasing the abrasion resistance without decreasing the toughness of WC–Co of a wide range of compositions and grain sizes. *Int. J. Refract. Met. Hard Mater.* **2007**, *25*, 57–61. https://doi.org/10.1016/j.ijrmhm.2005.11.015.
32. Gant, A.J.; Gee, M.G. Abrasion of tungsten carbide hardmetals using hard counterfaces. *Int. J. Refract. Met. Hard Mater.* **2006**, *24*, 189–198. https://doi.org/10.1016/j.ijrmhm.2005.05.007.
33. Gee, M.G.; Gant, A.; Roebuck, B. Wear mechanisms in abrasion and erosion of WC/Co and related hardmetals. *Wear* **2007**, *263*, 137–148. https://doi.org/10.1016/j.wear.2006.12.046.
34. Angseryd, J.; From, A.; Wallin, J.; et al. On a wear test for rock drill inserts. *Wear* **2013**, *301*, 109–115. https://doi.org/10.1016/j.wear.2012.10.023.
35. Grasser, D.; Gallo, S.C.; Pereira, M.; et al. Experimental investigation of the effect of insert spacing on abrasion wear resistance of a composite. *Wear* **2022**, *494*, 204277. https://doi.org/10.1016/j.wear.2022.204277.
36. Toller-Nordström, L.; Sten, S.; Kritikos, M.; et al. Wear properties of cemented carbides with new binder solutions for rock drilling inserts. *Wear* **2025**, *570*, 205909. https://doi.org/10.1016/j.wear.2025.205909.
37. Grejtak, T.; Kuns, M.W.; Lacey, J.A.; et al. Enhancing the shredder durability for biomass preprocessing by utilizing wear-resistant cutter materials. *Tribol. Int.* **2025**, *210*, 110766. https://doi.org/10.1016/j.triboint.2025.110766.
38. Saai, A.; Bjørge, R.; Dahl, F.; et al. Adaptation of Laboratory tests for the assessment of wear resistance of drill-bit inserts for rotary-percussive drilling of hard rocks. *Wear* **2020**, *456*, 203366. https://doi.org/10.1016/j.wear.2020.203366.
39. Tkalich, D.; Kane, A.; Saai, A.; et al. Wear of cemented tungsten carbide percussive drill–bit inserts: Laboratory and field study. *Wear* **2017**, *386*, 106–117. https://doi.org/10.1016/j.wear.2017.05.010.